Colorful methods to detect ion channels and pores: intravesicular chromogenic probes that respond to pH, pM and covalent capture†

Sara M. Butterfield, Andreas Hennig and Stefan Matile*

Received 6th January 2009, Accepted 18th February 2009
First published as an Advance Article on the web 17th March 2009
DOI: 10.1039/b900130a

The activity of synthetic pores, ion channels, transporters and carriers is usually determined with fluorescent probes in vesicles or by conductance measurements in planar lipid bilayers. Elaborating on more colorful alternatives, we here introduce 5(6)-carboxynaphthofluorescein (CNF) as an intravesicular pH probe for the colorimetric detection of activity, selectivity and cooperativity of ion channels such as gramicidin A. We further report that intravesicular pyrocatechol violet (PV), together with extravesicular Cu^{2+}, extravesicular 4-carboxyphenylboronic acid (CBA) or intravesicular 4-(benzyl-*N*-glutamate)boronic acid (BGBA) can detect the activity of synthetic pores or cell-penetrating peptide (CPP) sensors. Their response to analytes such as dodecylphosphate, hyaluronan or IP_6 are reported as high-contrast color changes from yellow to blue, from yellow to red, or from red to green.

Introduction

In routine assays,[1] the activity of synthetic pores, ion channels, transporters and carriers[2–16] is determined with a broad variety of fluorescent probes in vesicles or by conductance measurements in planar (black) or supported lipid bilayer membranes. These two complementary methods are most popular because they are informative, sensitive and adaptable to probe specific characteristics such as ion selectivity, voltage gating, ligand gating, blockage, and so on.[1] Several alternative methods exist as well. For example, ion selective electrodes have been used in vesicle assays despite limitations in sensitivity and adaptability. The use of NMR spectroscopy has been explored in several variations. Particular attention has been given to sodium NMR spectroscopy with shift reagent additives to discriminate between intra- and extravesicular sodium. Although appealing from a conceptual point of view, this method is rather slow, inflexible, insensitive and inadaptable to probe specific characteristics. Recently, G-quartets have been introduced as ECCD (exciton-coupled circular dichroism) probes for the detection of the activity of ion channels and pores by circular dichroism spectroscopy.[17,18]

With the recently emerging sensing and screening applications[19–27] in diagnostics and drug discovery, there is growing interest in the development of new methods in general and colorimetric approaches in particular to detect the activity of ion channels, transporters and pores with the naked eye. This is particularly true for the recent introduction of synthetic pores[23] and cell-penetrating peptides[27] as multianalyte sensors in complex matrices. Colorimetric detection is also of interest for the development of screening assays in drug discovery efforts to better target membrane proteins. Here, we report the identification and characterization of selected probes that respond to changes in pH and pM as well as to covalent capture.

Department of Organic Chemistry, University of Geneva, Geneva, Switzerland. E-mail: stefan.matile@unige.ch; Fax: +41 22 379 5123; Tel: +41 22 379 6523; Web: www.unige.ch/sciences/chiorg/matile/

† This paper is dedicated to Professor Seiji Shinkai in recognition of his contributions to supramolecular chemistry.

Results and discussion

pH Indicators

The detection of the activity of ion channels with pH probes is particularly attractive because they can report on transmembrane H^+/M^+- and OH^-/A^--antiport in a very general manner.[1] Loaded into vesicles, the velocity of the decay of an applied pH gradient in the presence and absence of an ion channel can be followed easily and continuously. High selectivities do not hinder detection because activity is not only observed for H^+/M^+- and OH^-/A^--antiport but also for symport or simple probe export.[1] Moreover, the detection of important characteristics such as anion/cation selectivity, ion selectivity sequences, voltage gating, ligand gating, blockage, catalysis, Hill plots and the dependence on surface potential, membrane composition, membrane fluidity, and so on is unproblematic with pH probes.[1] Only the detection of pH profiles is not straightforward. The most popular fluorescent pH probe is HPTS **1** (Fig. 1). With pK_a ~7.3 and two complementary excitation maxima, HPTS is perfect for ratiometric detection near neutral water (Fig. 1). Other common fluorescent pH probes include CF **2**, although alternative modes of operation are more common for this fluorophore (pK_a ~6.5).

From the rich collection of commercially available colorimetric pH indicators, the usefulness of Congo red and 5(6)-carboxynaphthofluorescein[28–30] (CNF, **3**, Fig. 1) to detect the activity of ion channels was explored first. Congo red was dropped quickly because loading into egg yolk phosphatidycholine large unilamellar vesicles (EYPC LUVs) was problematic.

Consistent with the literature, CNF changed the color from red to blue between pH 6 and pH 10 (Fig. 1). The emission around 668 nm increased with increasing pH. The pH profile confirmed a global $pK_a = 7.3 \pm 0.1$ in water. CNF was entrapped in EYPC LUVs using standard freeze–thaw–extrusion methods.

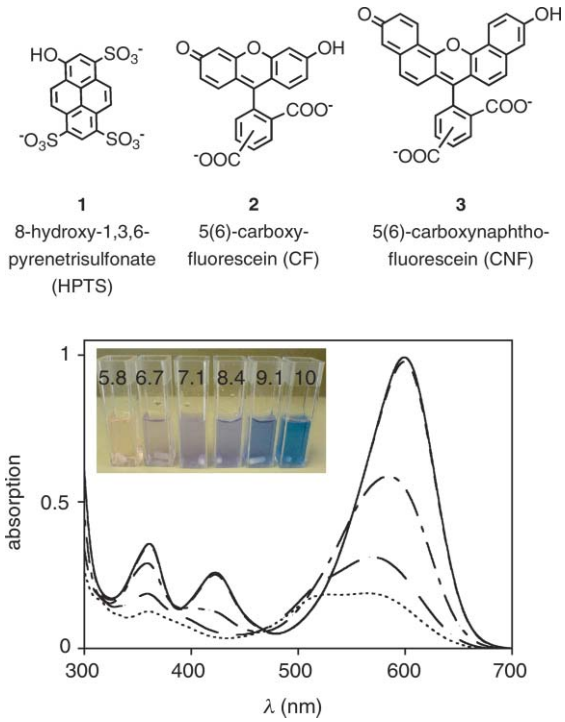

Fig. 1 The absorption spectrum and the color (inset) of CNF in water (24 μM) at pH 5.8 (dotted), 6.7, 7.1 8.4 and 9.1 (solid).

Extravesicular chromphores were removed by gel filtration. The obtained EYPC-LUVs⊃CNF were bluish.

The absorption of CNF at 598 nm was monitored continuously during the addition of first HCl, then gramicidin A (gA), and finally triton X-100 (tX) to EYPC-LUVs⊃CNF (Fig. 2A). Insensitivity toward the initial acid pulse confirmed that intravesicular CNF is inaccessible for extravesicular protons (Fig. 2A and 2E). Addition of gA, a classical model ion channel,[18,31,32] caused a decrease in blue absorption of CNF. This change was consistent with intravesicular acidification by proton/cation antiport. Final vesicle lysis with tX gave a pale pink color independent of sample history (Fig. 2E). This final step was essential to calibrate different experiments (Fig. 2A). The absorption at 598 nm after lysis was higher that the minimal values obtained with gA. This apparent influence of tX on optical probes is neither unique nor problematic. Namely, different experiments were first calibrated to identical maximal fractional absorption at the beginning of the experiment and identical minimal fractional absorption at 598 nm after vesicle lysis. In a second calibration step, all normalized curves were then adjusted to $A = 0$ at the beginning and $A = 1$ for the highest activity observed before lysis. This second recalibration reduced the uniformized fractional absorption after lysis to $A \sim 0.45$ (Fig. 2A).

Interference from vesicle light scattering is intrinsically irrelevant for qualitative detection of color changes with the naked eye. Eventual contributions to quantitative kinetics from light scattering require consideration for single-wavelength kinetics, whereas ratiometric double-channel kinetics are not affected. LUVs with a diameter of 100 nm produce significant light scattering at high energy only. Chromophores with red-shifted absorption were selected for this study to avoid any possible interference from light scattering.

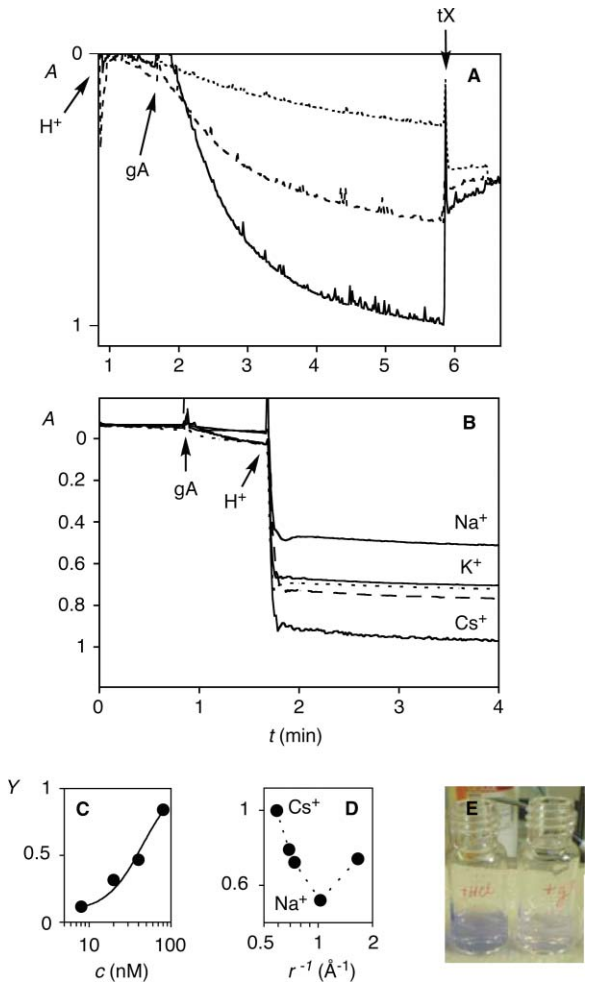

Fig. 2 (A) Fractional absorption A (λ 598 nm) during the addition of HCl (9 μl, 0.3 M aq, 50 s), gA (from 3 μM DMSO, 7.5 nM (dotted), 40 (dashed), and 80 nM (solid) final concentration) and tX (40 μl, 1.2% aq, 350 s) to EYPC-LUVs⊃CNF (12 mM CNF, 10 mM Tris, 80 mM NaCl, pH 9.1) in buffer (10 mM Tris, 107 mM NaCl, pH 9.1). (B) Same for the addition of gA (60 nM, 50 s) before HCl (100 s) with extravesicular MCl, M = Cs, Rb (dashed), K, Na, or Li (dotted). (C) Dependence of the fractional activity Y (initial velocity of change in absorption or final absorption before lysis) on the concentration of gA, with fit to Hill equation (from A). (D) Same for the reciprocal radius of the cation M in the extravesicular buffer (from B). (E) EYPC-LUVs⊃CNF after addition of HCl (left) and gA (right).

The colorimetric CNF assay was first used to record the dependence of the activity on the concentration of gA (Fig. 2A). The obtained dose response curve exhibited weak cooperativity (Fig. 2C). A Hill coefficient $n \sim 2$ was consistent with the endergonic self-assembly of gA into thermodynamically unstable dimers.[18,31,32]

The dependence of colorimetric CNF assay on the sequence of addition was explored next (Fig. 2A *vs.* 2B). Addition of gA before the acid pulse produced active channels that were naturally invisible (Fig. 2B). Application of an acid pulse to these preformed gA channels caused an instantaneous change in color (Fig. 2B). This fast response to an acid pulse applied to preformed channels differed clearly to the slow response that was observed when channel formation was initiated after the acid pulse. This difference confirmed that velocity of H^+/M^+-exchange through preformed

gA observed in the fast kinetics is far beyond the timescale of this experiment (Fig. 2B). The slow kinetics observed for channel formation after acid pulse reflects a slowly increasing number of gA-containing vesicles that is affected by many parameters including intravesicular transfer, self-assembly and ion selectivity of the final channel (Fig. 2A). Identical observations concerning sequence of addition have been made with the fluorometric pH probe HPTS.[33]

The detectability of the ion selectivity of gA channels with the colorimetric CNF assay was explored by extravesicular ion exchange. This method has been used before with the fluorometric HPTS assay.[1,34] Moreover, qualitative compatibility of the obtained values with permeability ratios from conductance measurements in planar bilayers has been confirmed.[34] With the colorimetric CNF assay, extravesicular cation exchange affected the apparent activity of gA channels in a meaningful manner (Fig. 2B). The obtained Eisenman selectivity topology I with a strong Li-anomaly was consistent with results from conductance experiments as well as fluorometric and chiroptical probes (Fig. 2D).[18,32]

pM Indicators

The use of cation complexing dyes to detect the activity of ion channels and pores is generally underexplored.[1] Initial screening revealed pyrocatechol violet (PV, **4**)[35–38] as preferable compared to the similarly functional pyrogallol red and arsenazo (III) for various reasons (Fig. 3). PV has been used previously to determine permeability[35] and composition[36] of lipid bilayer vesicles. Moreover, PV was of vital importance for the discovery of indicator displacement assays.[37,38] Cation screening for PV in neutral water revealed the highest contrast for the binding of Cu^{2+}, which occurred with a drastic change in color from yellow to blue.

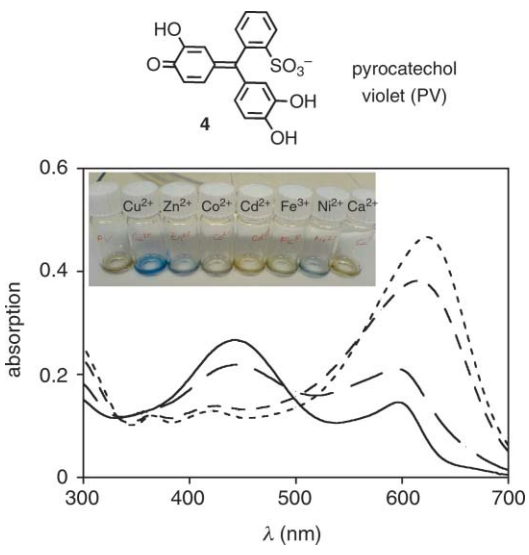

Fig. 3 The absorption spectrum of PV in water (24 μM) in the presence of 0 (solid), 10 (broken), 50 (dashed) and 100 μM Cu^{2+} (dotted, 10 mM Tris, 10 mM NaCl, pH 7.5). Inset: Color change of PV (100 μM) upon addition of cations (300 μM, 10 mM Tris, 10 mM NaCl, pH 7.5).

The pM indicator assay was developed in analogy to pH indicator assays, with intravesicular dyes meeting extravesicular cations instead of protons to cause a change in color. Different to the situation with protons, the detection of Cu^{2+} influx appeared too invasive to study ion channels. However, PV export and chromogenic binding to extravesicular Cu^{2+} appeared fully appropriate to detect activity, activation or inactivation of anion selective pores, anion transporters or simple vesicle destruction.

The colorimetric detection of pore activity was explored with synthetic pores **5**. These pores are formed by one of the best understood artificial β-barrels (Fig. 4).[21,23,24,39] Their cylindrical self-assembly is achieved by the interdigitation of peptide strands to form short amphiphilic β-sheets that position the non-planar rigid-rod *p*-octiphenyl scaffolds in close proximity.[40,41] The sequence of the short peptides is chosen to produce a hydrophobic barrel exterior and a cationic, functionalized interior. The former is thought to maximize interactions with the surrounding membrane, the latter to stabilize internal space and to recognize and translocate anionic analytes and probes such as PV.

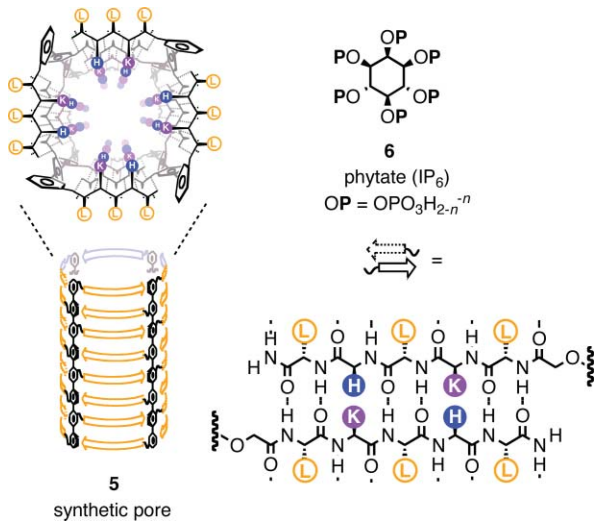

Fig. 4 Structure of pore **5** and pore inactivator **6**. In the rigid-rod β-barrel **5**, β-sheets are given as solid (backbone) and dotted lines (hydrogen bonds, *top*) or as arrows (N→C, *bottom*); external amino-acid residues are dark on white (L, leucine), internal residues are white on dark (K, lysine; H, histidine).

To explore the detectability of synthetic pore **5** at work with colorimetric pM indicators, PV was loaded into EYPC LUVs using routine freeze–thaw–extrusion methods, and extravesicular PV was removed by gel filtration. The obtained EYPC-LUVs⊃PV were yellow (Fig. 5D). To detect pore activity with EYPC-LUVs⊃PV, the change of the absorption at 612 nm was followed continuously during the addition of first $CuCl_2$, then pore **5**, and finally tX (Fig. 5A). Whereas the presence of $CuCl_2$ alone passed unnoticed by EYPC-LUVs⊃PV, the additional presence of pore **5** and tX was reported as a high-contrast color change from yellow to blue (Fig. 5D).

As with pH probes, the sequence of addition mattered with pM probes. The color change caused by Cu^{2+} addition after pore addition was much faster than that caused by pore addition after Cu^{2+} addition (Fig. 5B *vs.* 5A). The reasons for this drastic and informative dependence of kinetics in pM assays on the sequence of addition were as discussed above for the CNF assay. The strong dependence of assay kinetics on the sequence of addition did, however, not influence the observed final activities (Fig. 5A *vs.*

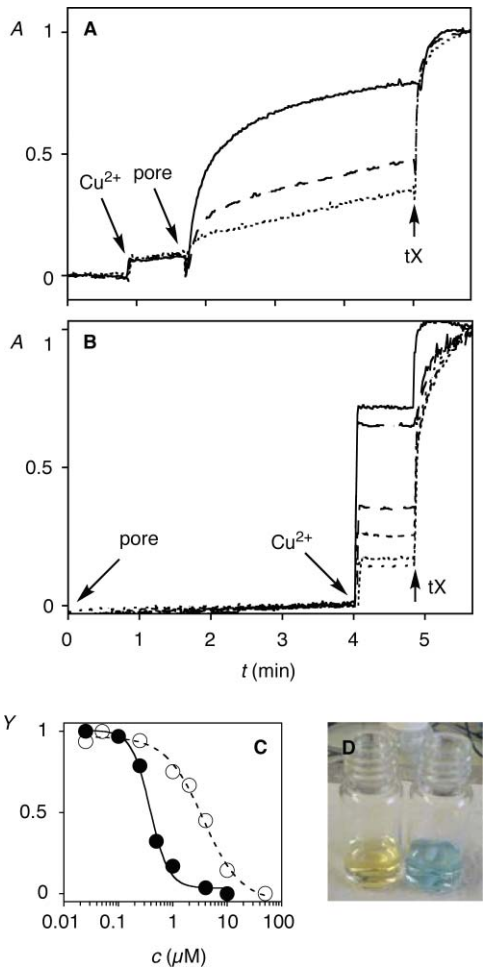

Fig. 5 (A) Fractional absorption A (λ 612 nm) during the addition of $CuCl_2$ (1.25 mM final, 50 s), **5** (180, 375 and 750 nM monomer, 100 s) and tX (40 μl, 1.2% aq, 350 s) to EYPC-LUVs⊃PV (2 mM PV, 10 mM Tris, 100 mM NaCl, pH 7.4) in buffer (10 mM Tris, 107 mM NaCl, pH 7.5). (B) Same for addition of **5** (750 nM monomer, 0 s) before $CuCl_2$ (313 μM, 240 s) in the presence of IP_6 (varied, see C). (C) Dose response curve for IP_6 for sequence of addition IP_6-**5**-Cu^{2+} (●, from B) and IP_6-Cu^{2+}-**5** (○, as in A). (D) EYPC-LUVs⊃PV after addition of Cu^{2+} (left) and tX (right).

5B, solid lines before 5 min). Identical observations concerning the independence of thermodynamics but not kinetics on the sequence of addition have been made and understood previously with conventional assays.[33]

The dependence of pore activity on the concentration of pore **5** was correctly reported by the PV/Cu assay (Fig. 5A). An EC_{50} ~400 nM was found (EC_{50} is the monomer concentration needed to obtain 50% activity for the tetrameric pore **5**). This value was similar to values obtained previously with conventional assays.[21,39]

Because of a central importance for sensing applications,[19–27] the colorimetric detection of the activation and inactivation of stimuli-responsive pores and transporters was of particular interest. In practice, inactivator efficiency is best described as reciprocal IC_{50}, the inactivator concentration needed to reduce pore activity to 50%. Phytate **6** was selected as a representative analyte of broad scientific importance.[24] With the conventional fluorogenic CF assay, phytate **6** inactivated pore **5** with an IC_{50} = 45 nM.[24] Colorimetric detection of the changes in activity of pore **5** in the presence of increasing phytate concentrations gave an $IC_{50} = 3.7 \pm 0.5$ μM (Fig. 5C, ○). This finding suggested that pore sensors that operate with the colorimetric PV/Cu assay would be about two orders of magnitude less sensitive than pore sensors that operate with the fluorometric CF assay. Similar losses in sensitivity with the PV/Cu assay were observed for pore inactivation by polyglutamate ($IC_{50} = 92 \pm 30$ μM) or hyaluronan ($IC_{50} = 10 \pm 1$ μg/ml).[39] However, the poor responsiveness of the PV/Cu assay was observed only when Cu^{2+} was added before the pore (Fig. 5A and 5C, ○). This observation suggested that binding of Cu^{2+} to the analytes reduces their affinity for the pore sensors. The poor responsiveness of the PV/Cu assay should thus be improvable by adding the pore before the Cu^{2+}, that is, reversal of the sequence of addition. This was found to be true. The efficiency of phytate **6** as inactivator of pore **5** improved almost 10-times to $IC_{50} = 385 \pm 30$ nM when Cu^{2+} was added after the pore (Fig. 5B and C, ●).

The compatibility of colorimetric PV/Cu assay with CPP-counteranion transporters was explored next. When activated by amphiphilic anions such as dodecylphosphate (DP), cell-penetrating peptides (CPPs)[42–51] such as polyarginine (pR) can efficiently mediate the export of fluorogenic anions such as CF from vesicles.[52–56] This counteranion-mediated activity is of use not only for cytosolic CPP delivery[57] but also for the development of cost-efficient multianalyte sensors, particularly for the otherwise problematic hydrophobic analytes.[22,27]

Used as described in the previous section with synthetic pores and their inactivators, the PV/Cu assay reported increasing pR activity with increasing DP concentrations (Fig. 6A). Hill analysis of the obtained dose response curve gave an $EC_{50} = 6.4 \pm 1.3$ μM for pR activation by DP (Fig. 6B). This value was in the range of the one determined for pR-DP complexes with the fluorogenic CF assay (19.0 ± 1.0 μM).[22] This independence of activator efficiencies on the assay system indicated that Cu^{2+} does not affect the interaction between pR and DP significantly.

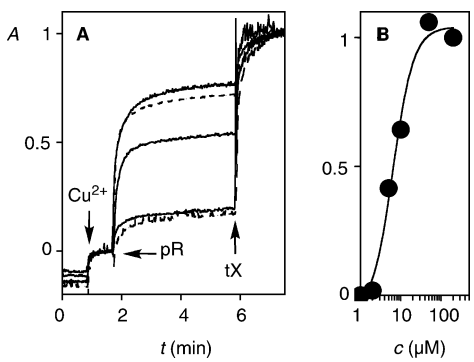

Fig. 6 (A) Fractional change in absorption A (λ 612 nm) during the addition of DP (0–200 μM final, <0 sec), $CuCl_2$ (313 μM, 50 s), pR (350 nM, 100 s) and tX (40 μl, 1.2% aq, 350 s) to EYPC-LUVs⊃PV (2 mM PV, 10 mM Tris, 100 mM NaCl, pH 7.5) in buffer (10 mM Tris, 107 mM NaCl, pH 7.5). (B) Dose response curve for DP.

The colorimetric PV/Cu assay is necessarily incompatible with the detection of pH profiles. Copper complexation by catechols is highly pH dependent, and insoluble hydroxides form under basic conditions. Both pH and copper concentration were kept unchanged in all studies for these reasons. The fraction of the released PV that is complexed by the excess of extravesicular

copper (1.25 mM) under these conditions was sufficient to cause the desired change in color and was not further quantified.

Covalent capture

Pioneering work by the Shinkai group contributed substantially to sensing applications of the covalent capture of catechols, α-hydroxy acids and vicinal diols by boronic acids.[25,26,58–69] Successful studies in several groups focused particularly on carbohydrate[60] and polyphenol[25] binding, applications in biology (aptamers, artificial amino acids)[67,68] and materials sciences (porous solids)[69] are currently emerging. Covalent capture by boronic acids has been used to inactivate synthetic pores.[25] However, reversible covalent capture by boronic acids has so far not been explored for the colorimetric detection of the activity of synthetic pores.

The color change of pyrocatechol violet (PV, **4**) in response to the reaction with boronic acids has been exploited in the Anslyn group to introduce indicator displacement assays to chemosensing.[37,38,63,64] 4-Carboxyphenylboronic acid (CBA, **7**) was selected as one of the simplest possible boronic acids with the negative charge needed to minimize passive diffusion through lipid bilayer membranes (Fig. 7). Addition of CBA to PV caused a high-contrast change in color from yellow to red (Fig. 7C). The dose response curve revealed an $EC_{50} = 333 \pm 17$ μM for dynamic covalent capture of PV by CBA at pH 7.5 (Fig. 7B). This value was as expected for the formation of boronate esters such as **8** with a $K_A \approx 3000$ M^{-1} under these conditions.[25,60,62]

To use the chromogenic reaction between catechol **4** and boronic acid **7** to detect pore activity, activation and inactivation with the naked eye, different approaches were conceivable. However, slow spontaneous release of intravesicular CBA was observed during the preparation of vesicles in the presence or the absence of co-entrapped PV. This finding established that in any practical assay, the still relatively hydrophobic CBA would have to be added extravesicularly to already made vesicles.

To use the chromogenic reaction between catechol **4** and boronic acid **7** to detect the activity of pores, vesicles were thus loaded with the unproblematic PV. The presence of extravesicular CBA above the $EC_{50} = 333 \pm 17$ μM did not change the yellow color of EYPC-LUVs⊃PV (Fig. 7C). The addition of pore **5** or tX, however, caused a high-contrast color change from yellow to red (Fig. 7C). This color change demonstrated the formation of boronic ester **8** after either efflux of intravesicular PV or influx of extravesicular CBA became possible. The change in color thus reflected the formation of pore **5** (or more complex events such as vesicle destruction).

To validate the PV/CBA assay, changes in absorption at 525 nm were detected continuously during the addition of synthetic pore **5** at different concentrations to EYPC-LUVs⊃PV in the presence of extravesicular CBA (Fig. 8A). Hill analysis of the obtained dose response curve gave an $EC_{50} = 350 \pm 30$ nM for the monomer concentration needed to obtain 50% activity of the tetrameric pore **5** (Fig. 8B, ●). Similarity of this value from the PV/CBA assay with values from the PV/Cu assay (above) and conventional assays[21,39] suggested that PV, boronic acid **7** and boronate ester **8** do not affect formation and activity of pore **5**.

According to the PV/CBA assay, inactivation of pore **5** by extravesicular phytate **6** occurred with an $IC_{50} = 600 \pm 100$ nM (Fig. 8C). This inactivator efficiency was better than the one obtained from the PV/Cu assay under similar conditions (Fig. 6C,

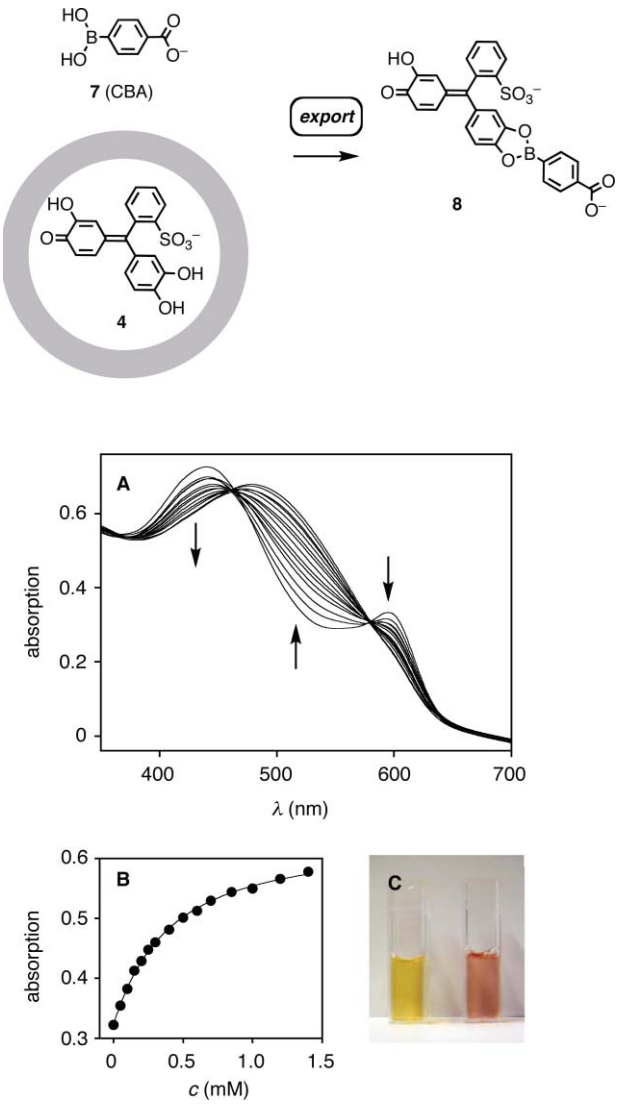

Fig. 7 (A) The absorption spectrum of PV (100 μM) in buffer (10 mM Tris, 100 mM NaCl, pH 7.5) in the presence of increasing concentrations of CBA. (B) Absorption (λ 525 nm) of PV as a function of the concentration of CBA. (C) EYPC-LUVs⊃PV after addition of CBA (1 mM, left) and tX (excess, right). Possible products of PV and CBA other than boronic ester **8** are not shown for clarity (*e.g.*, conjugate bases and dimers).

○, $IC_{50} = 3.7 \pm 0.5$ μM). The interaction between pore **5** and phytate **6** was thus less disturbed by extravesicular CBA than by extravesicular Cu^{2+}. In this example, the PV/CBA assay, based on covalent capture, is clearly preferable compared to the more interfering inorganic PV/Cu assay.

The colorimetric PV/CBA assay was not compatible with the colorimetric detection of CPP-counteranion transporters. In the presence of extravesicular CBA, pR transporters were active already without DP counterion activators (Fig. 9B, ○). Apparently, CBA can function as a pR activator. This interpretation appeared reasonable considering the negative charge and relative hydrophobicity of CBA. The slight increase in pR activity around 10 μM DP was consistent with activator exchange from CBA to DP (Fig. 9B, ○). The effective DP concentration roughly matched the $EC_{50} = 6.4 \pm 1.3$ μM found in the PV/Cu assay (Fig. 6B). Decreasing pR activity at excess activator has been observed before

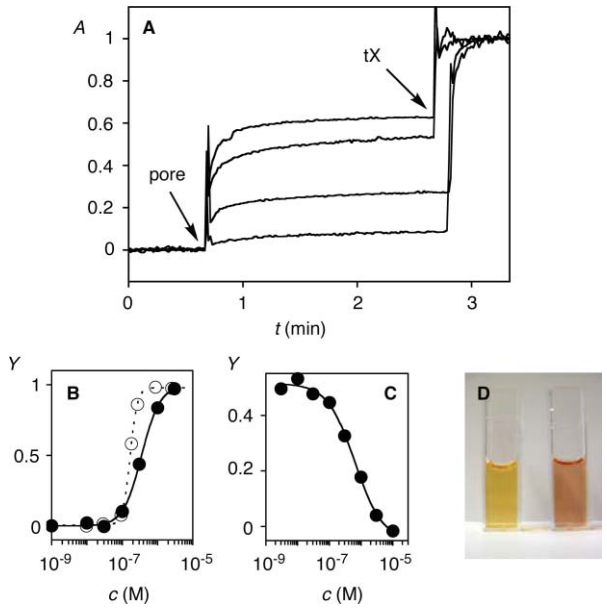

Fig. 8 (A) Fractional absorption A (λ 525 nm) during the addition of pore **5** (c in B) and tX (excess 40 µl) to EYPC-LUVs⊃PV (20 mM PV, 10 mM Tris, 70 mM NaCl, pH 7.5) in buffer (1 mM CBA, 10 mM Tris, 100 mM NaCl, pH 7.5). (B) Hill analysis of (A), reported as Y as a function of the monomer concentration c (>4-times c of the active tetramer, ●; compared to results in EYPC-LUVs⊃PV/BGBA, ○; see Fig. 9). (C) Dose response curve for IP_6 at constant concentration of pore **5** (800 nM monomer). (D) EYPC-LUVs⊃PV after addition of CBA and pore **5** in the presence (left) and absence (right) of IP_6 (200 µM).

(Fig. 9B, ○).[27,52–54] It occurs in response to the self-assembly of the amphiphilic DP monomers into hydrophilic DP micelles that bind pR strongly but avoid the membrane. The cmc of DP should thus be around ~200 µM.

pR-activation by the extravesicular boronic acid could be avoided if the latter could be loaded together with PV as red boronate ester **8** into the LUV. Interference-free extravesicular formation of pR-DP transporters should then mediate the export of intravesicular boronate ester **8**, which would hydrolyze upon dilution and afford the yellow PV together with the colorless CBA. To replace the slightly membrane permeable CBA with a more hydrophilic boronic acid, 4-(benzyl-*N*-glutamate)boronic acid (BGBA) **9** was prepared by reductive amination of 4-formylphenylboronic acid with glutamate. The preparation of EYPC-LUVs⊃PV/BGBA was unproblematic, the obtained vesicles were stable and could be used without any extra precaution. Addition of either DP or pR did not change the rusty color of intravesicular boronate ester **10** (Fig. 9A, solid; 9C, left). Addition of both DP and pR (Fig. 9A, dashed, 9C, middle) and the addition of tX (Fig. 9A, solid, 9C, left) caused a color change from rusty to olive. The dose response curve for pR activation with DP revealed the normal sigmoidal behavior centered at $EC_{50} = 6.8 \pm 0.4$ µM (Fig. 9B, ●). This demonstrated that, different to extravesicular CBA probes, intravesicular BGBA probes do not interfere with the activity of pR-DP transporters.

For completion, the Hill plot of pore **5** was also recorded EYPC-LUVs⊃PV/BGBA (Fig. 8B, ○). The colorimetric response obtained with intravesicular BGBA was similar to that with extravesicular CBA (Fig. 8B, ●) and other probes.[39] However,

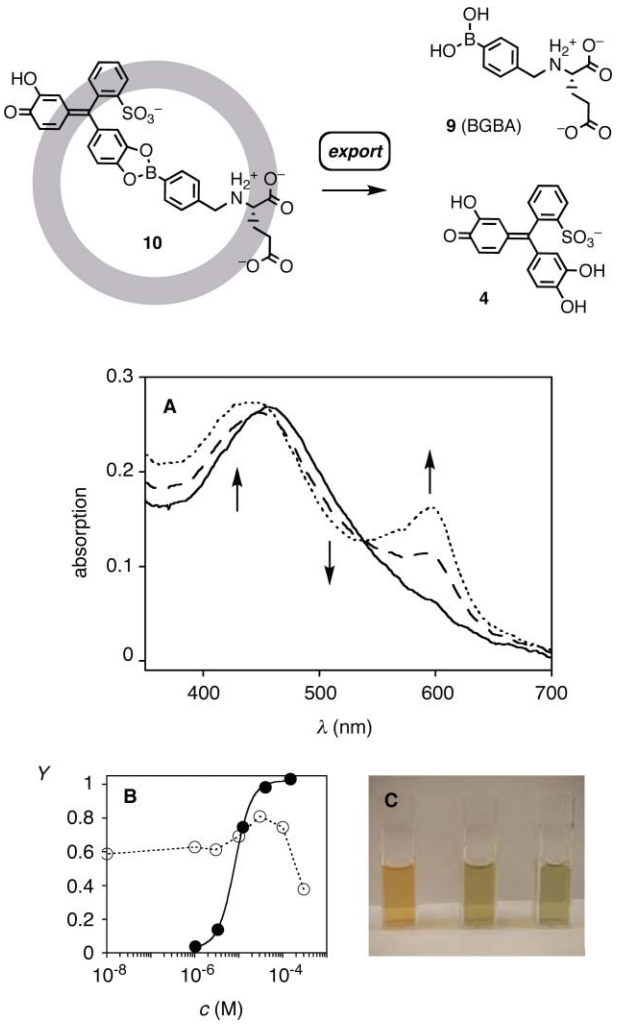

Fig. 9 (A) The absorption spectrum of EYPC-LUVs⊃PV/BGBA (200 µM) in buffer (1.8 ml, 10 mM Tris, 100 mM NaCl, pH 7.5) after the addition of DP (solid; 10 µM final), pR (dashed; 350 nM µM final) and excess tX (dotted). (B) Hill analysis of spectral changes as in A, measured at λ 600 nm and reported as Y as a function of DP concentration c at constant pR concentration (350 nM, ●; compared to results in EYPC-LUVs⊃PV and external CBA, ○; see Fig. 8). (C) EYPC-LUVs⊃PV/BGBA in the presence of pR (left), DP and pR (middle), and tX (right).

pore formation in EYPC-LUVs⊃PV/BGBA exhibited, with a Hill coefficient $n = 4.1 \pm 0.2$, higher apparent cooperativity than with extravesicular CBA ($n = 1.7 \pm 0.1$). Much experimental evidence from other studies support that pore **5** is a tetramer.[39–41] The difference found in cooperativity thus suggested that intravesicular BGBA interferes less with the self-assembly of pore **5** than extravesicular CBA. Many effects can naturally be imagined to account for the more subtle influence of extravesicular CBA on pore **5**.[70]

Conclusions

Four new methods to detect activity, activation, inactivation and selectivity of ion channels, transporters and pores with the naked eye are introduced. The four introduced methods use colorimetric probes that respond to pH, pM and covalent capture.

The CNF assay exhibits a color change from bluish to light pink. In the CNF assay, carboxynaphthofluorescein is used as an intravesicular pH probe to report on facilitated anion or cation exchange in response to an applied pH gradient. The CNF assay is the colorimetric version of the HPTS assay, that is arguably the most popular fluorometric assay to study activity and selectivity of ion channels.

The PV/Cu assay exhibits a color change from yellow to blue. This color change occurs when intravesicular pyrocatechol violet and extravesicular Cu^{2+} meet. Presumably less suitable for ion channels, the PV/Cu assay is of use to characterize pores and transporters and their response to chemical stimulation.

The PV/CBA assay exhibits a color change from yellow to red. It occurs when intravesicular PV and extravesicular 4-carboxyphenylboronic acid meet. Like the PV/Cu assay, the PV/CBA assay is of use to characterize stimuli-responsive pores and transporters.

The related PV/BGBA assay exhibits a color change from red to green. It occurs when the boronate ester formed between intravesicular PV and intravesicular BGBA hydrolyzes. This happens upon probe dilution when leaving the vesicles. The PV/BGBA assay is of use to characterize stimuli-responsive pores and transporters and is less interfering than the PV/CBA assay.

The difference between PV/Cu and PV/BGBA (or PV/CBA) assays is that the former operates with coordination chemistry between Cu^{2+} and catechols, whereas the latter use covalent capture between boronic acids and catechols. The PV/BGBA assay appears more robust than the PV/Cu and PV/CBA assays with regard to the use of pores as sensors because the intravesicular boronic acid interacts less than extravesicular Cu^{2+} or boronic acids with analytes such as phytate, activators such as dodecyl phosphate, synthetic pores or CPP transporters.

Taken together, the four introduced colorimetric assays operate in a complementary manner to satisfy complementary needs. They demonstrate that detection of activity, activation, inactivation and selectivity of ion channels, transporters and pores with the naked eye is possible and straightforward, identify a marvelous topic to enjoy creative supramolecular chemistry and illustrate much potential for future refinements toward the development of advanced screening and sensing devices.

Experimental part

Materials and methods

All compounds, probes, channels, transporters, analytes, buffers, salts, detergents, solvents, *etc*, were commercially available from standard suppliers except for pore **5**, which was synthesized following previously reported procedures.[39] EYPC was from Avanti Polar Lipids. UV-vis spectra were measured on a Varian Cary 1 Bio spectrophotometer equipped with a magnetic stirrer and a temperature controller (25 °C).

4-(Benzyl-*N*-glutamate)boronic acid (BGBA, 9)

Glutamic acid (466 mg, 3.17 mmol) was suspended in H_2O (8 ml), and 10 M aqueous NaOH (0.32 ml, 3.20 mmol) was added to yield a clear solution. Addition of 4-formylphenylboronic acid (475 mg, 3.17 mmol) in MeOH (8 ml) at rt caused immediate precipitation. Addition of $NaBH_3CN$ (256 mg, 4.08 mmol) in MeOH (2 ml) gave a clear solution. The reaction mixture was stirred at room temperature. After ~1 h, precipitation of a colorless solid could be observed. The reaction mixture was stirred for an additional 48 h, while the pH was carefully maintained at pH 7 by stepwise addition of 1 M HCl (1.2 ml). Subsequently, the precipitate is filtered through a Büchner funnel and washed with acetone. Drying under high vacuum yielded 412 mg (46%) of pure **9** as a colorless solid. Mp: 231–232 °C; IR (neat): 3190 (br), 2952 (w), 2923 (w), 1645 (m), 1631 (m), 1572 (s), 1471 (m), 1388 (s), 1210 (m); ^{1}H NMR (400 MHz, D_2O): 7.78 (d, ^3J = 7.8 Hz, 2H), 7.46 (d, ^3J = 8.1 Hz, 2H), 4.15–4.26 (m, 2H), 3.57–3.59 (m, 1H), 2.25–2.39 (m, 2H), 2.00–2.05 (m, 2H); ^{13}C NMR (100 MHz, D_2O): 181.3 (s), 173.5 (s), 134.2 (d), 133.3 (s), 129.2 (d), 62.0 (d), 50.1 (t), 33.9 (t), 26.0 (t); MS (ESI, MeOH–H_2O 9 : 1): 280 (100, $[M - H]^-$).

EYPC-LUVs⊃CNF

Solutions of EYPC in $CHCl_3$–MeOH 1 : 1 (25 µl, 1.0 g/ml) were dried under vacuum (>2 h) to give a transparent thin film. Hydration with "inside" buffer (12 mM CNF, 10 mM Tris, 80 mM NaCl, pH 9.1) for 1 h was followed by several freeze–thaw cycles (5×) and extrusions (>10×, mini-extruder with a stacked polycarbonate membrane of pore size 100 nm, Avanti). External CNF was removed by gel filtration (Sephadex G-50) with "outside" buffer (10 mM Tris, 107 mM MCl, pH 9.1; M = Cs, Rb, K, Na, or Li). The LUV fractions were combined and diluted to 6 ml. Final conditions: ~2.5 mM EYPC; inside: 12 mM CNF, 10 mM Tris, 80 mM NaCl, pH 9.1; outside: 10 mM Tris, 107 mM MCl, pH 9.1; M = Cs, Rb, K, Na, or Li.

CNF assay

EYPC-LUVs⊃CF (750 µl) were added to gently stirred buffer in a thermostated cuvette (1250 µl; 10 mM Tris, 107 mM MCl, pH 9.1; M = Cs, Rb, K, Na, or Li). Absorption A_t (λ = 598 nm) was monitored as a function of time (t) during the addition of HCl (9 µl, 0.5 M aq, t = 50 or 100 s, external pH ~6.5), gA (c variable, 3 µM DMSO, t = 50 or 100 s) and tX (40 µl, 1.2% aq, t = 350 s).

CV/Cu assay

EYPC-LUVs⊃CV were prepared following above procedure for EYPC-LUVs⊃CNF. Final conditions: ~2.5 mM EYPC; inside: 2 mM PV, 10 mM Tris, 100 mM NaCl, pH 7.5; outside: 10 mM Tris, 107 mM NaCl, pH 7.5. EYPC-LUVs⊃CV (200 µl) were added to gently stirred buffer in a thermostated cuvette (1800 µl; 10 mM Tris, 107 mM NaCl, pH 7.5, activator (DP; c variable) or inactivator (IP_6, pE, hyaluronan; c variable)). Absorption A_t (λ = 612 nm) was monitored as a function of time (t) during the addition of $CuCl_2$ (10 µl, 250 mM DMSO, t = 50 or 240 s), pore **5** (c variable, 37.5 µM DMSO, t = 100 or 0 s) or pR (350 nM aq, t = 100 s) and tX (40 µl, 1.2% aq, t = 350 s).

CV/CBA assay

EYPC-LUVs⊃CV were prepared following above procedure for EYPC-LUVs⊃CNF. Final conditions: ~2.5 mM EYPC; inside: 20 mM PV, 10 mM Tris, 70 mM NaCl, pH 7.5; outside: 10 mM Tris, 100 mM NaCl, pH 7.5. EYPC-LUVs⊃CV (200 µl) were

added to gently stirred buffer in a thermostated cuvette (1800 µl; 1 mM CBA, 10 mM Tris, 100 mM NaCl, pH 7.5, activator (DP; *c* variable) or inactivator (IP_6; *c* variable)). Absorption A_t ($\lambda = 525$ nm) was monitored as a function of time (*t*) during the addition of pore **5** (*c* variable, *t* ~ 50 s) or pR (350 nM aq, *t* ~ 50 s) and tX (40 µl, 1.2% aq, *t* ~ 160 s).

CV/BGBA assay

EYPC-LUVs⊃CV/BGBA were prepared following above procedure for EYPC-LUVs⊃CNF. Final conditions: ~2.5 mM EYPC; inside: 20 mM PV, 20 mM BGBA, 10 mM Tris, 40 mM NaCl, pH 7.5; outside: 10 mM Tris, 100 mM NaCl, pH 7.5. EYPC-LUVs⊃CV/BGBA (200 µl) were added to gently stirred buffer in a thermostated cuvette (1800 µl; 10 mM Tris, 100 mM NaCl, pH 7.5). Absorption spectra were monitored before and after the addition of first activator (DP in DMSO; *c* variable) or inactivator (IP_6; *c* variable), then pR (350 nM aq) or pore **5** (*c* variable), and finally tX (40 µl, 1.2% aq, *t* ~ 160 s).

Data analysis

Absorption kinetics were normalized to fractional absorption *A* applying eqn (1)

$$A = \{(A_t - A_0)/(A_\infty - A_0)\}/\{(A_t^{MAX} - A_0)/(A_\infty - A_0)\} \quad (1)$$

where $A_0 = A_t$ at channel addition, $A_\infty = A_t$ after final lysis, and A_t^{MAX} = maximal A_t before final lysis. From the obtained curves, fractional activities *Y* were determined with eqn (2)

$$Y = (Y_{MAX} - Y_{MAX(0)})/(Y_{MAX(\infty)} - Y_{MAX(0)}) \quad (2)$$

where Y_{MAX} is *A* after a constant period of time after channel addition (typically ~2 min), $Y_{MAX(0)}$ is Y_{MAX} for lowest activity and $Y_{MAX(\infty)}$ is Y_{MAX} for the highest activity ($Y = 1$) for a given experiment (*e.g.*, $Y_{MAX(\infty)} = Y_{MAX}$ with Cs^+, $Y_{MAX(0)} = Y_{MAX}$ without gA in Fig. 3B). For Hill analysis of channels/pores, *Y* was plotted against the monomer concentration $c_{MONOMER}$ and fitted to the Hill eqn (3) to give the effective concentration EC_{50} and the Hill coefficient *n*.

$$Y = Y_\infty + (Y_0 - Y_\infty)/\{1 + (c_{MONOMER}/EC_{50})^n\} \quad (3)$$

where Y_0 is *Y* in the absence of channels/pores, Y_∞ is *Y* with excess channels/pores (*e.g.*, Fig. 2B).

For Hill analysis of activators, *Y* was plotted against the activator concentration $c_{ACTIVATOR}$ and fitted to the Hill eqn (4) to give the effective concentration EC_{50} and the Hill coefficient *n*.

$$Y = Y_\infty + (Y_0 - Y_\infty)/\{1 + (c_{ACTIVATOR}/EC_{50})^n\} \quad (4)$$

where Y_0 is *Y* in the absence of activators, Y_∞ is *Y* with excess activators (*e.g.*, Fig. 7B).

For Hill analysis of inactivators, *Y* was plotted against the inactivator concentration $c_{INACTIVATOR}$ and fitted to the Hill eqn (5) to give the inhibitory concentration IC_{50} and the Hill coefficient *n*.

$$Y = Y_\infty + (Y_0 - Y_\infty)/\{1 + (c_{INACTIVATOR}/IC_{50})^n\} \quad (5)$$

where Y_0 is *Y* in the absence of inactivators, Y_∞ is *Y* with excess inactivators (*e.g.*, Fig. 6C).

Acknowledgements

We thank D.-H. Tran for contributions to synthesis, D. Jeannerat, A. Pinto and S. Grass for NMR measurements, and P. Perrottet, N. Oudry and G. Hopfgartner for MS measurements. This work was supported by the University of Geneva and the Swiss NSF.

References

1 S. Matile and N. Sakai, The Characterization of Synthetic Ion Channels and Pores, in *Analytical Methods in Supramolecular Chemistry*, C. A. Schalley, Ed., Wiley, Weinheim, 2007, 391–418.
2 W. H. Binder, *Angew. Chem. Int. Ed.*, 2008, **47**, 3092–3095.
3 P. Davis, D. N. Sheppard and B. D. Smith, *Chem. Soc. Rev.*, 2007, **36**, 348–357.
4 T. M. Fyles, *Chem. Soc. Rev.*, 2007, **36**, 335–347.
5 P. A. Gale, *Acc. Chem. Res.*, 2006, **39**, 465–475.
6 A. L. Sisson, M. R. Shah, S. Bhosale and S. Matile, *Chem. Soc. Rev.*, 2006, **35**, 1269–1286.
7 U. Koert, L. Al-Momani and J. R. Pfeifer, *Synthesis*, 2004, **8**, 1129–1146.
8 S. Matile, A. Som and N. Sordé, *Tetrahedron*, 2004, **60**, 6405–6435.
9 G. W. Gokel and A. Mukhopadhyay, *Chem. Soc. Rev.*, 2001, **30**, 274–286.
10 A. Satake, M. Yamamura, M. Oda and Y. Kobuke, *J. Am. Chem. Soc.*, 2008, **130**, 6314–6315.
11 L. Ma, M. Melegari, M. Colombini and J. T. Davis, *J. Am. Chem. Soc.*, 2008, **130**, 2938–2939.
12 C. P. Wilson and S. J. Webb, *Chem. Commun.*, 2008, 4007–4009.
13 I. Izzo, S. Licen, N. Maulucci, G. Autore, S. Marzocco, P. Tecilla and F. De Riccardis, *Chem. Commun.*, 2008, 2986–2988.
14 M. Jung, H. Kim, K. Baek and K. Kim, *Angew. Chem. Int. Ed.*, 2008, **47**, 5755–5757.
15 X. Li, B. Shen, X. Q. Yao and D. Yang, *J. Am. Chem. Soc.*, 2007, **129**, 7264–7265.
16 P. L. Boudreault and N. Voyer, *Org. Biomol. Chem.*, 2007, **5**, 1459–1465.
17 N. Sakai and S. Matile, *Chirality*, 2003, **15**, 766–771.
18 A. Hennig and S. Matile, *Chirality*, 2008, **20**, 932–937.
19 S. Matile, H. Tanaka and S. Litvinchuk, *Top. Curr. Chem.*, 2007, **277**, 219–250.
20 G. Das, P. Talukdar and S. Matile, *Science*, 2002, **298**, 1600–1602.
21 S. Litvinchuk, N. Sordé and S. Matile, *J. Am. Chem. Soc.*, 2005, **127**, 9316–9317.
22 T. Miyatake, M. Nishihara and S. Matile, *J. Am. Chem. Soc.*, 2006, **128**, 12420–12421.
23 S. Litvinchuk, H. Tanaka, T. Miyatake, D. Pasini, T. Tanaka, G. Bollot, J. Mareda and S. Matile, *Nat. Mater*, 2007, **6**, 576–580.
24 S. M. Butterfield, D.-H. Tran, H. Zhang, G. D. Prestwich and S. Matile, *J. Am. Chem. Soc.*, 2008, **130**, 3270–3271.
25 S. Hagihara, H. Tanaka and S. Matile, *J. Am. Chem. Soc.*, 2008, **130**, 5656–5657.
26 S. Hagihara, H. Tanaka and S. Matile, *Org. Biomol. Chem.*, 2008, **6**, 2259–2262.
27 S. M. Butterfield, T. Miyatake and S. Matile, *Angew. Chem. Int. Ed.*, 2009, **48**, 325–328.
28 O. S. Wolfbeis, *Mikrochim. Acta*, 1992, **108**, 133–141.
29 A. Song, S. Parus and R. Kopelman, *Anal. Chem.*, 1997, **69**, 863–867.
30 M. Ramanathan and A. L. Simonian, *Biosens. Bioelectr.*, 2007, **22**, 3001–3007.
31 A. M. O'Connell, R. E. Koeppe, II and O. S. Andersen, *Science*, 1990, **250**, 1256–1259.
32 A. Vescovi, A. Knoll and U. Koert, *Org. Biomol. Chem.*, 2003, **1**, 2259–2262.
33 V. Gorteau, G. Bollot, J. Mareda and S. Matile, *Org. Biomol. Chem.*, 2007, **5**, 3000–3012.
34 N. Sakai, D. Houdebert and S. Matile, *Chem. Eur. J*, 2003, **9**, 223–232.
35 Y. Jin, M. Li and X. Hou, *J. Pharm. Biomed. Anal.*, 2005, **37**, 379–382.
36 R. G. Hanshaw, E. J. O'Neil, M. Foley, R. T. Carpenter and B. D. Smith, *J. Mater. Chem.*, 2005, **15**, 2707–2713.
37 L. Zhu, Z. Zhong and E. V. Anslyn, *J. Am. Chem. Soc.*, 2005, **127**, 4260–4269.
38 L. Zhu and E. V. Anslyn, *J. Am. Chem. Soc.*, 2004, **126**, 3676–3677.

39 S. Litvinchuk, G. Bollot, J. Mareda, A. Som, D. Ronan, M. R. Shah, P. Perrottet, N. Sakai and S. Matile, *J. Am. Chem. Soc.*, 2004, **126**, 10067–10075.
40 N. Sakai, J. Mareda and S. Matile, *Acc. Chem. Res*, 2005, **38**, 79–87.
41 N. Sakai, J. Mareda and S. Matile, *Acc. Chem. Res*, 2008, **41**, 1354–1365.
42 I. Nakase, T. Takeuchi, G. Tanaka and S. Futaki, *Adv. Drug Del. Rev.*, 2008, **60**, 598–607.
43 K. M. Stewart, K. L. Horton and S. O. Kelley, *Org. Biomol. Chem.*, 2008, **6**, 2242–2255.
44 A. Verma, O. Uzun, Y. H. Hu, Y. Hu, H. S. Han, N. Watson, S. L. Chen, D. J. Irvine and F. Stellacci, *Nat. Mater*, 2008, **7**, 588–595.
45 B. A. Smith, D. S. Daniels, A. E. Coplin, G. E. Jordan, L. M. McGregor and A. Schepartz, *J. Am. Chem. Soc.*, 2008, **130**, 2948–2949.
46 E. K. Esbjorner, P. Lincoln and B. Norden, *Biochem. Biophys. Acta*, 2007, **1768**, 1550–1558.
47 S. M. Fuchs and R. T. Raines, *ACS Chem. Biol.*, 2007, **2**, 167–170.
48 T. Shimanouchi, P. Walde, J. Gardiner, Y. R. Mahajan, D. Seebach, A. Thomae, S. D. Kraemer, M. Voser and R. Kuboi, *Biochem. Biophys. Acta*, 2007, **1768**, 2726–2736.
49 M. Tang, A. J. Waring and M. Hong, *J. Am. Chem. Soc.*, 2007, **129**, 11438–11446.
50 E. A. Goun, T. H. Pillow, L. R. Jones, J. B. Rothbard and P. A. Wender, *ChemBioChem*, 2006, **7**, 1497–1515.
51 S. Pujals, J. Fernandez-Carneado, C. Lopez-Iglesias, M. J. Kogan and E. Giralt, *Biochem. Biophys. Acta*, 2006, **1758**, 264–279.
52 N. Sakai and S. Matile, *J. Am. Chem. Soc.*, 2003, **125**, 14348–14356.
53 F. Perret, M. Nishihara, T. Takeuchi, S. Futaki, A. N. Lazar, A. W. Coleman, N. Sakai and S. Matile, *J. Am. Chem. Soc.*, 2005, **127**, 1114–1115.
54 M. Nishihara, F. Perret, T. Takeuchi, S. Futaki, A. N. Lazar, A. W. Coleman, N. Sakai and S. Matile, *Org. Biomol. Chem.*, 2005, **3**, 1659–1669.
55 N. Sakai, T. Takeuchi, S. Futaki and S. Matile, *ChemBioChem*, 2005, **6**, 114–122.
56 A. Hennig, G. J. Gabriel, G. N. Tew and S. Matile, *J. Am. Chem. Soc.*, 2008, **130**, 10338–10344.
57 T. Takeuchi, M. Kosuge, A. Tadokoro, Y. Sugiura, M. Nishi, M. Kawata, N. Sakai, S. Matile and S. Futaki, *ACS Chem. Biol.*, 2006, **1**, 299–303.
58 T. D. James, K. R. A. S. Sandanayake and S. Shinkai, *Angew. Chem. Int. Ed.*, 1994, **33**, 2207–2209.
59 T. D. James, K. R. A. S. Sandanayake and S. Shinkai, *Nature*, 1995, **374**, 345–347.
60 T. D. James, *Top. Curr. Chem.*, 2007, **277**, 107–152.
61 J. Yoon and A. W. Czarnik, *Bioorg. Med. Chem.*, 1993, **1**, 267–271.
62 G. Springsteen and B. Wang, *Tetrahedron*, 2002, **58**, 5291–5300.
63 N. Y. Edwards, T. W. Sager, J. T. McDevitt and E. V. Anslyn, *J. Am. Chem. Soc.*, 2007, **129**, 13575–13583.
64 S. L. Wiskur, J. J. Lavigne, A. Metzger, S. L. Tobey, V. Lynch and E. V. Anslyn, *Chem. Eur. J.*, 2008, **10**, 3792–3804.
65 M. Maue and T. Schrader, *Angew. Chem. Int. Ed.*, 2005, **44**, 2265–22670.
66 P. J. Duggan, T. A. Houston, M. J. Kiefel, S. M. Levonis, B. D. Smith and M. L. Szydzik, *Tetrahedron*, 2008, **64**, 7122–7126.
67 M. Li, N. Lin, Z. Huang, L. Du, C. Altier, H. Fang and B. Wang, *J. Am. Chem. Soc.*, 2008, **130**, 12636–12638.
68 E. Brustad, M. L. Bushey, J. W. Lee, D. Groff, W. Liu and P. G. Schultz, *Angew. Chem. Int. Ed.*, 2008, **47**, 8220–8223.
69 H. M. El-Kaderi, J. R. Hunt, J. L. Mendoza-Cortés, A. P. Côté, R. E. Taylor, M. O'Keeffe and O. M. Yaghi, *Science*, 2007, **316**, 268–272.
70 S. Bhosale and S. Matile, *Chirality*, 2006, **18**, 849–856.

